Received: 13 August 2024 | Revised: 22 December 2024 | Accepted: 16 January 2025

DOI: 10.1002/alz.70018

Alzheimer's & Dementia®
THE JOURNAL OF THE ALZHEIMER'S ASSOCIATION

RESEARCH ARTICLE

Relationships between hypometabolism and both β-amyloid and tau PET in corticobasal syndrome

Alma Ghirelli[1,2,3] | Austin W. Goodrich[4] | Yehkyoung C. Stephens[1] | Jonathan Graff-Radford[1] | Farwa Ali[1] | Mary M. Machulda[5] | Chistopher G. Schwarz[6] | Matthew L. Senjem[6,7] | Federica Agosta[2,3,8] | Massimo Filippi[2,3,8] | Clifford R. Jack Jr.[6] | Val J. Lowe[6] | Keith A. Josephs[1] | Jennifer L. Whitwell[6]

[1]Department of Neurology, Mayo Clinic, Rochester, Minnesota, USA

[2]Neuroimaging Research Unit, Division of Neuroscience, IRCCS San Raffaele Scientific Institute, Milan, Italy

[3]Neurology Unit, IRCCS San Raffaele Scientific Institute, Milan, Italy

[4]Department of Quantitative Health Sciences, Mayo Clinic, Rochester, Minnesota, USA

[5]Department of Psychiatry and Psychology, Mayo Clinic, Rochester, Minnesota, USA

[6]Department of Radiology, Mayo Clinic, Rochester, Minnesota, USA

[7]Department of Information Technology, Mayo Clinic, Rochester, Minnesota, USA

[8]Vita-Salute San Raffaele University, Milan, Italy

Correspondence
Jennifer L. Whitwell, Department of Radiology, Mayo Clinic, 200 1st St SW, Rochester, MN 55905, USA.
Email: Whitwell.jennifer@mayo.edu

Funding information
National Institutes of Health, Grant/Award Number: R01-AG50603,R01-NS112153,R01-NS89757

Abstract

INTRODUCTION: Alzheimer's disease (AD) pathology causes corticobasal syndrome (CBS) in 21%–50% of patients. Studies have assessed hypometabolism in CBS according to β-amyloid (A) positron emission tomography (PET), but the understanding of the association of both AD-tau (T) and A with hypometabolism is incomplete.

METHODS: Thirty-three CBS patients and 45 controls underwent fluorodeoxyglucose (FDG), flortaucipir, and Pittsburgh compound-B PET and were classified as A± and T±. FDG-PET uptake was extracted for 12 regions-of-interest in dominant (most affected) and non-dominant hemispheres and compared across A/T groups.

RESULTS: A+T+ patients had greater hypometabolism in temporo-parieto-occipital cortices than A+T- and A-T- groups, with no differences observed between the A+T- and A-T- groups. FDG asymmetry was more accentuated in A+T+ patients. Medial temporal and basal ganglia metabolism were similar across AT groups.

DISCUSSION: Amyloid and tau positivity contribute synergistically to hypometabolism and asymmetry in temporo-parieto-occipital cortices in CBS, with AD-like patterns of hypometabolism observed only in A+T+ patients.

KEYWORDS
Alzheimer's disease, corticobasal syndrome, FDG-PET, flortaucipir PET, PiB-PET

Highlights

- Amyloid (A) and tau PET (T) status can be used to stratify CBS patients.
- A+T+ CBS patients show more hypometabolism in temporo-parieto-occipital cortices.
- Medial temporal metabolism (typical AD pattern) is similar across AT groups.
- Parieto-occipital cortices should be assessed when investigating AT pathology in CBS.
- Amyloid and tau positivity contribute synergistically to hypometabolism and asymmetry in CBS.

1 | INTRODUCTION

Corticobasal syndrome (CBS) is characterized by progressive and asymmetric cortical and extrapyramidal deficits, including parkinsonism, ideomotor limb apraxia, cortical sensory deficits, alien limb phenomenon, myoclonus, and dystonia.[1] The most common underlying pathology of CBS is corticobasal degeneration (CBD), but other pathologies such as progressive supranuclear palsy (PSP) and Alzheimer's disease (AD) have been described, as well as the TAR DNA binding protein of 43 kDa (TDP-43).[2] While CBD is the most common pathology, accounting for approximately 37% of cases, AD pathology has been reported in 21 to 50% of cases.[3–8] Furthermore, in cases in which AD does not represent the primary pathology, AD co-pathology has frequently been observed, with most patients featuring either Braak neurofibrillary tangle II or Braak III tau stages.[3,5–7]

From a clinical standpoint, patients with CBS due to pathologically confirmed AD (CBS-AD) often have myoclonus, visuospatial/perceptual symptoms, ideomotor apraxia, or episodic memory loss, while features of PSP and apraxia of speech are less common.[3,9] On neuroimaging, CBS is characterized by asymmetric atrophy and/or hypometabolism on 18F fluorodeoxyglucose (FDG) positron emission tomography (PET) in posterior frontal and parietal lobes, which is greater in the hemisphere contralateral to the most affected limb (i.e., dominant hemisphere).[10] CBS-AD is associated with an accentuated asymmetric atrophy and hypometabolism in temporal, parietal, and occipital lobes, while CBS-TDP is associated with prefrontal atrophy, CBS-CBD a more focal involvement of posterior frontal lobes, and CBS-PSP mild cortical involvement with some midbrain atrophy.[3,11]

Studies have also used β-amyloid PET to provide a biomarker diagnosis of AD in cases of CBS. These studies have reported β-amyloid PET positivity (A+) in 13%–44% of CBS patients and found greater atrophy and hypometabolism in the temporal, parietal, and occipital lobe in the A+ patients.[3,11,12] Magnetic resonance imaging (MRI) has been reported to have a sensitivity of 73% and a specificity of only 46% in predicting A+ status,[13] while FDG-PET in different studies had a sensitivity of 78%–91% and an inconsistent specificity of 50%–100%.[13,14] Some studies have analyzed tau PET imaging in patients with CBS. Flortaucipir (FTP), a radiotracer for tau, has been demonstrated to bind primarily to paired helical filaments (3R + 4R) tau, that is, AD-tau,[15] with less sensitivity to detect 4R tau, typical of PSP and CBD pathology,[16] or TDP43.[17,18] Mild FTP PET uptake that is thought to reflect 4R tau is typically observed in the premotor/motor and frontal cortices in CBS,[19–21] while striking FTP uptake is observed in the temporal lobes in AD.[15] Therefore, FTP, particularly in the temporal lobes, is considered an accurate in vivo biomarker of AD paired helical filament tau. Hence, patients with positive β-amyloid PET and temporal lobe tau PET can be considered to have biomarker confirmed AD.[22] Studies have assessed tau PET patterns in CBS patients classified by β-amyloid PET. In one study, tau PET uptake was more pronounced in the dorsolateral prefrontal cortex in A+ compared to A-CBS patients, providing a sensitivity of 91% for β-amyloid positivity.[23] However, not all A+ CBS cases also show tau PET uptake, particularly in AD-related regions[23,24]; hence, it is not clear that it is appropriate to use only β-amyloid PET to assess *ante mortem* impact of AD in CBS.

Different studies have analyzed how molecular PET uptake varies across AD and non-AD pathology in CBS patients, but the role of the synergistic effect of both tau and β-amyloid positivity in determining cortical hypometabolism has yet to be fully unraveled. The aims of this work, therefore, were to evaluate clinical features, regional metabolism, and asymmetry across CBS patients defined either using only β-amyloid PET or using both β-amyloid and tau PET.

RESEARCH IN CONTEXT

1. **Systematic review**: The literature was reviewed using PubMed. Although AD pathology accounts for approximately 37% of CBS cases, no study has systematically analyzed the combined effects of PiB and flortaucipir uptake on the pattern of FDG-PET hypometabolism in CBS patients.
2. **Interpretation**: We found that CBS patients can be stratified according to their amyloid and tau status on PET, as they carry a different pattern and severity of hypometabolism, which becomes more severe, widespread, and lateralized in patients with both amyloid and tau positivity, demonstrating in vivo that amyloid and tau synergistically act on the neurodegenerative processes.
3. **Future directions**: Future studies featuring confirmatory *post mortem* pathology should clarify the role of amyloid and tau PET in classifying CBS patients and validate the pattern of asymmetric parieto-occipital hypometabolism as a potential in vivo biomarker of AD pathology.

2 | METHODS

2.1 | Subjects

A total of 33 patients who met probable or possible criteria for CBS[1] were recruited by the Neurodegenerative Research Group (NRG) at Mayo Clinic between May 2016 and September 2023, and had undergone FDG PET, [18F]FTP tau PET, and PiB PET during the same visit. The NRG (PIs: Whitwell/Josephs) has been enrolling and following patients with neurodegenerative syndromes including CBS for more than a decade. A thorough neurological and neuropsychological evaluation was conducted. Parkinsonism was evaluated using the Movement Disorders Society sponsored revision of the Unified Parkinson's Disease Rating Scale Part III (MDS-UPDRS III),[25] eye saccade abnormalities were evaluated using the PSP Saccadic Impairment Scale,[26] and ideomotor praxis was evaluated with the Test for Upper Limb Apraxia (TULIA)[27] as well as with the Western Aphasia Battery (WAB) – praxis subtest.[28] General cognition was tested with the Mon-

treal Cognitive Assessment (MoCA),[29] memory was assessed with the Camden face and Camden words tests,[30] while visuospatial and perception functions with Incomplete Letters and Cube Analysis from the Visual Object and Space Perception (VOSP) battery.[31] A total of 45 healthy controls with similar age and sex were enrolled and underwent the same protocol.

2.2 | PET acquisition and analysis

All PET scans were acquired using a PET/CT scanner (GE Healthcare, Milwaukee, Wisconsin) operating in 3D mode, as previously described.[32,33] FDG, PiB, and flortaucipir images were co-registered to the MPRAGE using 6 degrees-of-freedom registration in SPM12 (fil.ion.ucl.ac.uk/spm/software/spm12/). All voxels in the MPRAGE space FDG-PET images were divided by the median uptake in the pons using the Mayo Clinic Adult Lifespan Template (MCALT) atlas to create standardized uptake value ratio (SUVR) images. Similarly, all voxels in the MPRAGE-space flortaucipir and PiB images were divided by median uptake in the cerebellar crus gray matter to create SUVR images. For PiB-PET, a global PiB SUVR was calculated as previously described, and we used a cut-point of 1.48 to define PiB-PET (A) positivity,[22] that is, 22 centiloids.[34] For tau-PET, we utilized a temporal meta-region-of-interest (ROI) described[35] to determine a positive status. Notwithstanding the knowledge that CBD-AD patients are characterized by a more widespread cortical uptake of flortaucipir,[36] in the absence of a specific cortical ROI to detect CBS-AD and in order to be as sensitive as possible to detect AD-related tau, the temporal meta-ROI was adopted. The temporal meta-ROI has been shown to have excellent sensitivity and specificity to separate AD pathology from CBD, PSP, and TDP-43 pathology.[36] For flortaucipir PET (T) positivity, we first explored two different cut points of 1.29 and 1.43.[37] The lower cutoff was previously determined by a neuropathological study,[15] while the upper cutoff was determined by Jack et al.[37] as the lower quartile of the meta-ROI SUVR of a cohort of AD patients with Braak stage III–IV. Since two patients had borderline tau positivity (Figure 1), we decided to adopt the stricter cutoff of 1.43, favoring increased specificity in determining T positivity. Asymmetry in both the PiB PET global SUVR (A) and FTP temporal meta-ROI (T) was also assessed by comparing uptake in the dominant (i.e., most affected) and non-dominant (i.e., less affected) hemispheres.

All MPRAGE scans were normalized to the MCALT and segmented (in their native space) via unified segmentation[38] with MCALT priors/settings.[15,22,37] The MCALT atlas was used to assess FDG-PET SUVR in 12 ROIs selected since they are expected to be involved in CBS across different pathologies: supplementary motor area (SMA), precentral, postcentral, superior parietal, medial temporal (amygdala, hippocampus, entorhinal cortex, parahippocampal gyrus), medial parietal, lateral temporal, lateral occipital, inferior parietal, superior frontal, middle frontal, and basal ganglia (caudate, putamen, globus pallidus).[11] Cortical regions were favored over subcortical regions given their preferential involvement in CBS-AD.[3] The ROI-specific difference of FDG uptake between the dominant and non-dominant hemispheres was also calculated, resulting in an ROI-specific asymmetry index. Figure S1 reports hemispheric FDG uptake values (dominant and non-dominant) across individual CBS patients for demonstration purposes. Analyses were performed without partial volume correction (PVC).

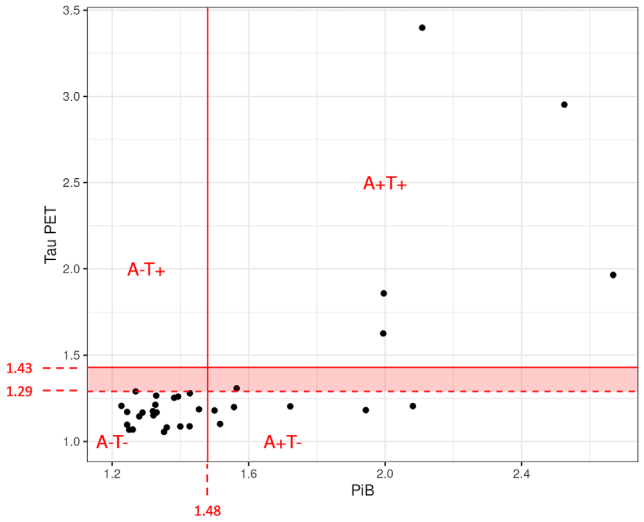

FIGURE 1 Distribution of CBS patients according to A/T status. The *x*-axis displays PiB SUVR values, while the *y*-axis displays flortaucipir SUVR values. Continued red lines represent SUVR cutoffs used for this study. The dotted red line represents the less strict flortaucipir cutoff for demonstrative purposes. CBS, corticobasal syndrome; PiB, Pittsburg compound B; SUVR, standardized uptake value ratio.

FDG-PET scans of a subset of four patients with different A/T statuses (N = 1 A-T-, N = 1 A+T-, N = 2 A+T+) were selected and presented in terms of statistical maps showing regions of significant hypometabolism relative to age-matched controls (GE Cortex ID) to demonstrate differences in asymmetry across A/T statuses (Figure S2).

Voxel-wise *t*-tests in SPM12 were used to compare uptake at FDG-PET for each AT group compared to controls. Results were assessed at family-wise error (FWE) $p < 0.05$.

2.3 | Statistical analysis

Continuous demographic and clinical variables were compared across CBS patients with a different A or A/T status using the Kruskal–Wallis rank sum test, while categorical variables were compared using Pearson's chi-squared tests. We used the Wilcoxon paired signed rank test to assess the difference between dominant and non-dominant FDG measurements within each brain ROI across CBS patients. Estimated marginal means were used to adjust for the effect of age when assessing A and T status on FDG-PET uptake. The resulting *p*-values and confidence intervals were adjusted using the Bonferroni correction to account for multiple comparisons. A *p*-value cutoff of < 0.05 was set to determine statistical significance. Analyses were carried out with R 4.2.2. The emmeans package was used to calculate the estimated marginal means and resulting contrasts with Bonferroni-corrected *p*-values and 95% confidence intervals.

TABLE 1 Demographic and clinical characteristics of patients divided by A status and controls.

Parameter	CBS total (*N* = 33)	CBS A- (*N* = 21)	CBS A+ (*N* = 12)	Control (*N* = 45)	*p*-value*
Sex (female)	16 (48.5%)	8 (38.1%)	8 (66.7%)	32 (71.1%)	0.114[a]
Dominant hemisphere (left)	12 (36.4%)	8 (42.1%)	4 (36.4%)	–	0.757[a]
Education	16.0 (12.5, 16.0)	14 (12, 16)	16 (14, 16)	16 (16, 18)	0.396[b]
Age of onset	63.5 (60.3, 69.2)	63.4 (60.9, 70.1)	65.6 (59.3, 68.2)	–	0.967[b]
Age at PET	69.0 (62.9, 72.2)	66.8 (62.6, 72.4)	66.5 (62.6, 70.4)	66.1 (61.5, 70.3)	0.708[b]
Disease duration (years)	2.6 (2.0, 3.4)	2.4 (1.9, 3.3)	3 (2.0, 4.1)	-	0.386[b]
MoCA	21.0 (17.5, 24.0)	23 (18.0, 25.0)	18 (15.0, 20.8)	26 (26.0, 28.0)	0.068[b]
UPDRS III	32.0 (23.8, 44.0)	33 (24.5, 44.0)	31 (24.5, 41.5)	0 (0.0, 2.0)	0.839[b]
WAB praxis	49.5 (43.8, 53.5)	52 (50, 55)	44 (41, 44)	60 (58, 60)	**0.027**[b]
TULIA	7.5 (3.5, 9.8)	8 (5.0, 10.0)	3.5 (1.5, 6.0)	NA	0.109[b]
PSIS	1.5 (0.2, 3.0)	1.5 (0.2, 3.0)	1.5 (0.8, 2.2)	0 (0.0, 0.0)	0.895[b]
Saccadic impairment**	18 (50%)	9 (50%)	2 (50%)	-	1.000
VOSP letters	20.0 (19.0, 20.0)	20 (19, 20)	20 (19, 20)	NA	0.602[b]
VOSP cubes	9.0 (8.0, 10.0)	9 (8, 10)	9 (8, 10)	NA	0.927[b]
Camden faces	22.0 (21.5, 23.5)	22 (21.5, 24.0)	22.5 (21.2, 23.0)	NA	0.683[b]
Camden words	24.0 (20.5, 24.0)	24 (22, 24)	20 (20, 22)	NA	0.444[b]
PiB SUVR	1.4 (1.3, 1.5)	1.3 (1.3, 1.4)	2 (1.6, 2.1)	1.4 (1.3, 1.5)	**0.001**[b]
Tau SUVR	1.2 (1.1, 1.2)	1.2 (1.1, 1.2)	1.3 (1.2, 1.9)	1.2 (1.1, 1.3)	**0.005**[b]
PiB asymmetry index (dominant–non dominant)	−0.0 (-0.1, 0.0)	−0.02 (−0.04, 0.02)	−0.07 (−0.15, −0.01)	–	0.116[b]
Tau asymmetry index (dominant–non dominant)	0.0 (−0.0, 0.0)	0.01 (−0.01, 0.03)	0.00 (−0.02, 0.10)	–	0.880[b]

Note: Data are shown as number (%), median (IQR). Bold values indicate significant results.
Abbreviations: CBS, corticobasal syndrome; IQR, interquartile range; MoCA, Montreal Cognitive Assessment; NA, not available; PiB, Pittsburg compound B; PSIS, PSP Saccadic Impairment Scale; SUVR, standardized uptake value ratio; TULIA, test for upper limb apraxia; UPDRS, Unified Parkinson's Disease Rating Scale; VOSP, Visual Object and Space Perception; WAB, Western Aphasia Battery.
[a]Pearson's chi-squaredd test.
[b]Kruskal–Wallis rank sum test.
**p*-value refers to A- vs. A+ CBS patients.
**Defined as PSIS ≥ 2.

3 | RESULTS

3.1 | Results by β-amyloid status

3.1.1 | Demographic and clinical characteristics

Out of the 33 patients with CBS in our cohort, 12 were classified as A+, and the remaining 21 were A-. No differences in sex, education, age of onset, age at MRI, and disease duration were observed between A+ and A- patients (Table 1). There were also no differences between A+ and A- patients for global cognition, visuospatial function, visual, or verbal memory. The A+ patients performed more poorly on the praxis subset of the WAB ($p = 0.027$), but degree of parkinsonism (measured with the MDS-UPDRS-III test) and saccadic impairment test did not significantly differ by A status. No significant differences in asymmetry were observed for the PiB global SUVR or temporal lobe FTP meta-ROI.

3.1.2 | FDG uptake across brain regions

Figure 2 and Table S1 show FDG uptake in the 12 A+ and 21 A- patients across the 12 ROIs for both dominant and non-dominant hemispheres. In the dominant hemisphere, lower FDG-PET SUVRs were observed in the superior parietal ($p = 0.02$) and postcentral ($p = 0.02$) cortices in A+ compared to A- patients. There was also a trend for significance in the inferior parietal cortex ($p = 0.079$). None of the other nine ROIs showed significant differences in FDG-PET metabolism for either the dominant or non-dominant hemisphere.

3.1.3 | Asymmetry of FDG uptake across brain regions according to A status

As shown in Figure 3 and Table S2, A+ patients demonstrated higher levels of asymmetry (larger differences between the dominant hemi-

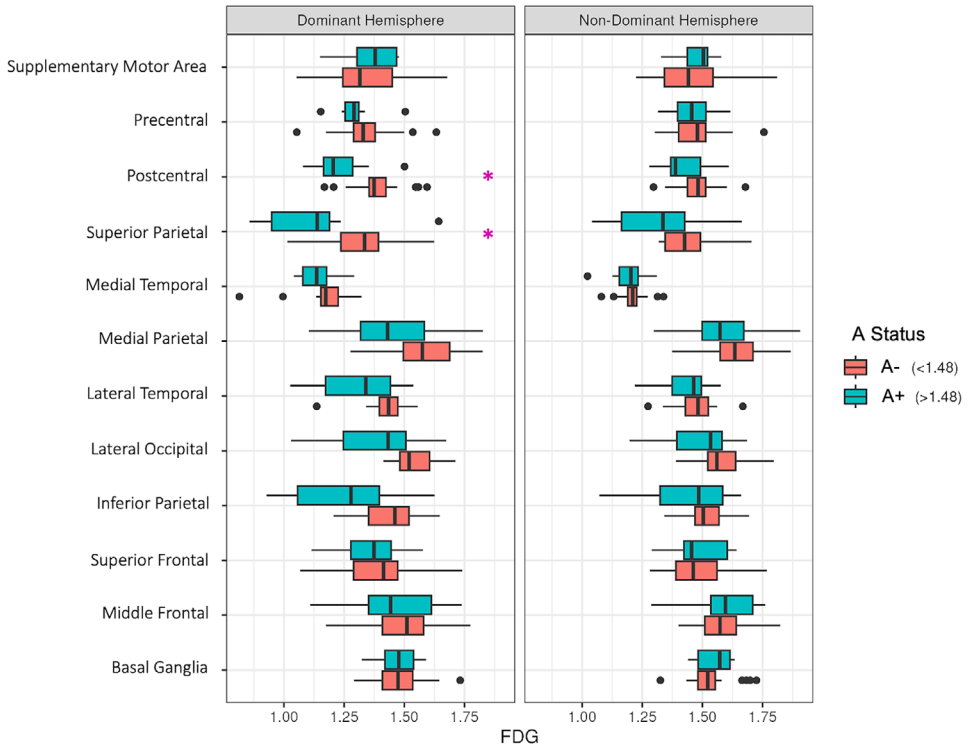

FIGURE 2 FDG uptake across different brain regions in A+ and A- CBS patients. Boxplots of FDG uptake (x-axis) according to A status (orange: A-, blue A+) determined by PiB PET. Data are shown per each hemisphere (dominant and non-dominant). Pink asterisks highlight significant differences. CBS, corticobasal syndrome; FDG, [18F] fluorodeoxyglucose; PiB, Pittsburg compound B.

sphere and non-dominant hemisphere FDG PET) compared to A- patients in the inferior parietal ($p = 0.017$), lateral temporal ($p = 0.012$), medial parietal ($p = 0.004$), superior parietal ($p = 0.015$), and postcentral ($p < 0.001$) cortices.

3.2 | Results across A and T status

Using the thresholds discussed in the methods section, patients were categorized into three AT groups: A-T- ($n = 21$), A+T- ($n = 7$), and A+T+ ($n = 5$) (Figure 1). Based on the chosen cutoffs, no patient was classified as A-T+.

3.2.1 | Demographic and clinical characteristics according to A and T status

Table 2 shows demographic and clinical characteristics for each AT combination. Sex, education, disease duration, and age at MRI did not differ across AT groups. Age of onset was lower in A+T+ patients compared to other groups ($p = 0.049$). No evidence of a difference in terms of neuropsychological and clinical metrics was appreciated across groups, with only a trend for differences in MoCA and WAB praxis, with worse performance in the A+T+ patients. Also in this case, no significant differences in asymmetry were observed for the PiB global SUVR or temporal lobe FTP meta-ROI.

3.2.2 | FDG uptake across brain regions according to A and T status

Figure 4 and Table S3 present data on FDG uptake in the three AT groups by hemisphere (dominant and non-dominant). Lower FDG-PET SUVRs were observed in A+T+ patients in the inferior parietal ($p = 0.002$), medial parietal ($p = 0.003$), superior parietal ($p < 0.001$), postcentral ($p < 0.001$), lateral occipital ($p = 0.002$), and lateral temporal cortices ($p = 0.005$) compared to the two other groups. Also, in the non-dominant hemisphere, A+T+ patients showed lower FDG-PET SUVRs compared to the other groups in the inferior parietal ($p = 0.002$), medial parietal ($p = 0.037$), superior parietal ($p = 0.002$), postcentral ($p = 0.053$), and lateral occipital cortices ($p = 0.033$). To better characterize the pattern of hypometabolism in each subgroup, Figure S3 shows voxel-level maps of hypometabolism across AT groups.

3.2.3 | Asymmetry of FDG uptake across brain regions according to A and T status

As shown in Figure 5 and Table S4, A+ T+ patients demonstrated higher levels of asymmetry (larger differences between the dominant hemisphere and non-dominant hemisphere FDG PET) compared to the other AT categories in the middle frontal ($p = 0.049$), postcentral ($p = 0.004$), superior parietal ($p = 0.052$), medial parietal ($p = 0.002$),

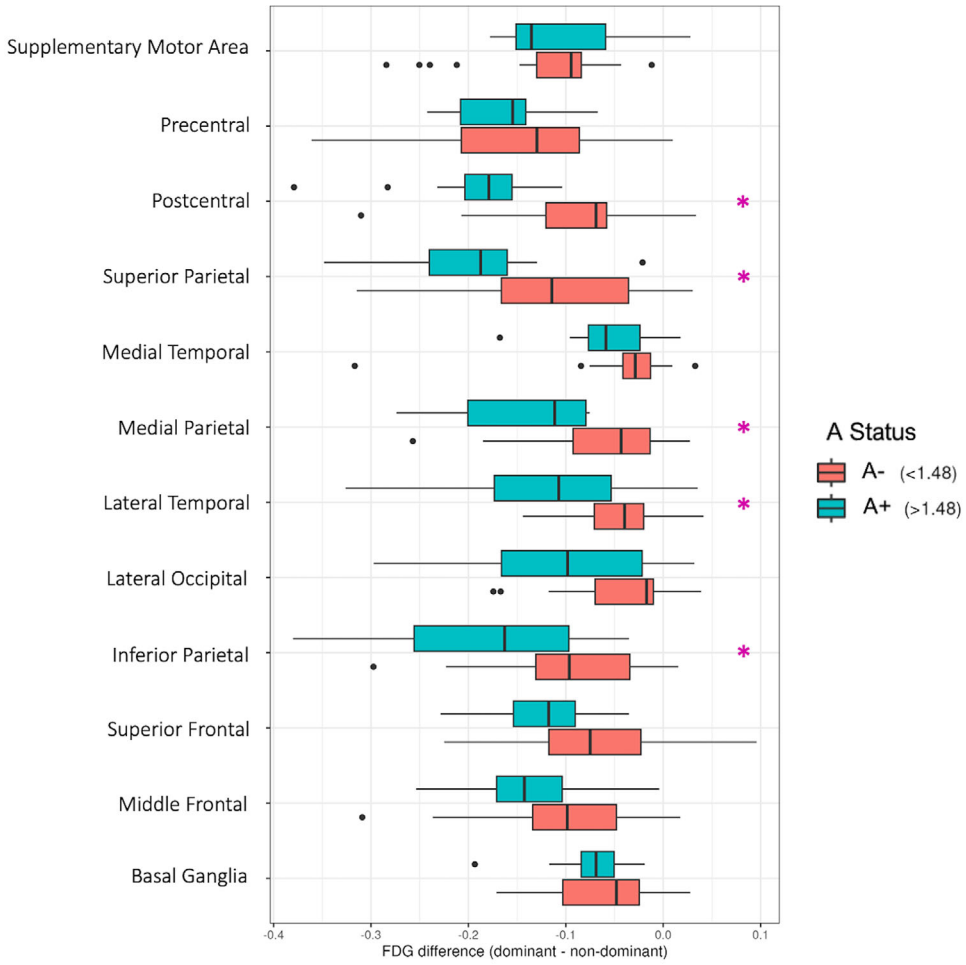

FIGURE 3 Asymmetry of FDG uptake in CBS patients according to A status. Boxplots represent the difference in FDG uptake (dominant–non-dominant hemisphere) according to A status (orange: A-; blue: A+) determined at PiB PET. Pink asterisks highlight significant differences. CBS, corticobasal syndrome; FDG, [18F] fluorodeoxyglucose; PET, positron emission tomography; PiB, Pittsburg compound B.

lateral temporal ($p = 0.005$), lateral occipital ($p = 0.006$), and inferior parietal ($p = 0.050$) cortices.

3.3 | Effects of age, A and T on FDG uptake

Age-corrected pairwise comparisons across AT groups are shown in Figure 6. In the dominant hemisphere, FDG-PET SUVR was lower in the A+T+ group compared to both the A+T- and A-T- groups in lateral occipital, lateral temporal, medial parietal, inferior parietal, middle frontal, superior parietal, and postcentral cortices (Figure 6A). Similarly, in the non-dominant hemisphere, lower FDG-PET SUVRs were observed in the A+T+ group compared to both the A+T- and A-T- groups in lateral temporal, medial parietal, inferior parietal, lateral occipital, and superior parietal cortices (Figure 6B). For asymmetry, the A+T+ group had a more asymmetric pattern of hypometabolism compared to both other groups in middle frontal, superior frontal, inferior parietal, lateral occipital, lateral temporal, medial parietal, medial temporal, and postcentral cortices (Figure 6C).

4 | DISCUSSION

In this study, we assessed how positivity on β-amyloid and tau PET influenced the pattern and extent of hypometabolism on FDG-PET in a cohort of CBS patients. After classifying patients according to their β-amyloid status alone, we observed greater hypometabolism in the postcentral and superior parietal cortices of the dominant hemisphere in the A+ group. However, when the cohort was stratified by both β-amyloid and tau PET status, the A+T+ group showed greater hypometabolism and greater asymmetry across all cortical ROIs compared to both the A+T- and A-T- groups. Hence, only the A+T+ group showed an FDG-PET profile consistent with that expected in CBS patients with AD.[3,11]

When our analysis was stratified by both A and T status, differences in FDG-PET uptake were striking, A+T+ patients showing greater hypometabolism in parieto-occipital cortices, middle frontal, lateral temporal, and postcentral cortices in the dominant hemisphere compared to both the A+T- and A-T- patients, with no differences observed between the A+T- and A-T- groups. The A+T+ patients also showed

TABLE 2 Demographic and clinical characteristics of patients according to A/T status.

Parameter	A-T- (*N* = 21)	A+T- (*N* = 7)	A+T+ (*N* = 5)	*p*-value
Sex (female)	8 (38.1%)	5 (71.4%)	3 (60%)	0.266[a]
Education	14.5 (12, 16)	16 (13, 16)	16 (15.5, 17)	0.455[b]
Age of onset	63.4 (60.9, 70.1)	68 (65.8, 69.6)	59.3 (56.4, 60.9)	**0.049**[b]
Age at PET	68.4 (63.2, 72.6)	70.3 (70.1, 73.3)	62.6 (62.5, 63,1)	0.124[b]
Disease duration (years)	2.4 (1.9, 3.3)	3.4 (2.5, 4.1)	2 (1.2, 3.3)	0.275[b]
MoCA	23 (18.0, 25.0)	18 (18.0, 22)	13 (11, 16.5)	0.081[b]
UPDRS III	33 (24.5, 44.0)	29 (25.2, 37.5)	31 (27, 41)	0.975[b]
WAB praxis	52 (49.8, 55)	46 (46, 46)	43 (38.5, 43.5)	0.074[b]
TULIA	8 (5.0, 10.0)	3.5 (1.5, 6.0)	NA	NA
PSIS	1.5 (0.2, 3.0)	1.5 (0.8, 2.3)	NA	NA
VOSP letters	20 (19, 20)	20 (19.3, 20)	19 (19, 19)	0.461[b]
VOSP cubes	9 (8, 10)	9.5 (8.8, 10)	6 (6, 6)	0.352[b]
Camden faces	22 (21.5, 24.0)	22.5 (21.2, 23.0)	NA	NA
Camden words	24 (21.5, 24)	20.5 (19.5, 22)	NA	NA
PiB asymmetry index (dominant–non dominant)	−0.02 (−0.04, 0.02)	−0.09 (−0.22, −0.01)	−0.04 (−0.07, −0.01)	0.264[b]
Tau asymmetry index (dominant–non dominant)	0.01 (−0.01, 0.03)	−0.01 (−0.02, 0.01)	0.10 (−0.08, 0.20)	0.251[b]

Note: Data shown as number (%), median (IQR). Bold values indicate significant results.
Abbreviations: CBS, corticobasal syndrome; IQR, interquartile range; MoCA, Montreal Cognitive Assessment; NA, not available; PiB, Pittsburg compound B; PSIS, PSP Saccadic Impairment Scale; SUVR, standardized uptake value ratio; TULIA, test for upper limb apraxia; UPDRS, Unified Parkinson's Disease Rating Scale; VOSP, Visual Object and Space Perception; WAB, western aphasia battery.
[a]Pearson's chi-squared test.
[b]Kruskal–Wallis rank sum test.

greater hypometabolism in the lateral temporal and parietal cortices of the non-dominant hemisphere. Our findings confirm the results of previous autopsy studies that demonstrated a temporo-parietal pattern of hypometabolism in CBS-AD patients on both FDG-PET[3,39] and SPECT.[12] Only the dominant parietal hemisphere showed increased hypometabolism when patients were stratified solely by A status, and it is clear from our findings that these weaker differences are driven by the fact that the A+T- patients do not show any differences in metabolism from the A-T- patients. It is, therefore, possible that either the clinical presentation in the A+T- patients is not driven by underlying AD or that FDG-PET is insensitive to early β-amyloid only in these patients. The A+T- patients were almost 10 years older than the A+T+ patients, suggesting that these patients may have age-associated β-amyloid deposition, or pathological aging.[40] A previous study carried out on normal older adults and patients with preclinical AD demonstrated that the combination of cortical amyloid and tau positivity on molecular PET (but not individual amyloid or tau PET) correlated with hypometabolism in the posterior cingulate, and this predicted memory decline.[41] Given that our cohort was relatively small, we cannot exclude that this could have affected the detection of hypometabolism in the A+T- group.

Moreover, we demonstrated that asymmetry in hypometabolism was globally more accentuated in A+T+ patients in parietal, lateral temporal, and occipital cortices, compared to the A+T- and A-T- groups. Hence, it appears as though AD pathology not only increases degeneration of the cortex but also increases the degree of asymmetry in AD-susceptible regions in CBS. In order to help readers visualize these differences, four selected FDG-PET scans from patients with different A/T statuses were selected, showing increased hypometabolism but, most strikingly, increased asymmetry when both amyloid and tau PET are positive (Figure S2). It is notable that we did not observe any differences by AT status in metabolism or asymmetry of the medial temporal lobe, basal ganglia, or precentral cortex. In contrast to the hippocampal involvement typically seen in the classical clinical presentation of AD, CBS-AD generally spares the hippocampus. Instead, it primarily affects the parieto-occipital cortices and lateral temporal areas.[39] At neuropathology, fewer neurofibrillary tangles are present in the hippocampi of AD-CBS patients compared to patients with AD pathology and classical memory impairments.[9] The lack of relationships to AT in the basal ganglia and precentral cortex likely reflects the fact that these regions are more typically targeted by CBD pathology, rather than AD. Our findings highlight the importance of examining the lateral temporal and occipital cortices when investigating AT pathology in CBS patients. These results, therefore, pave the way for future research to explore the role of temporo-occipital regions in studying AD pathology in CBS rather than the classical temporal meta-ROI.

The synergistic action of β-amyloid and tau has been consistently demonstrated. A recent study on cerebrospinal fluid (CSF) neurodegenerative biomarkers demonstrated a correlation between longitu-

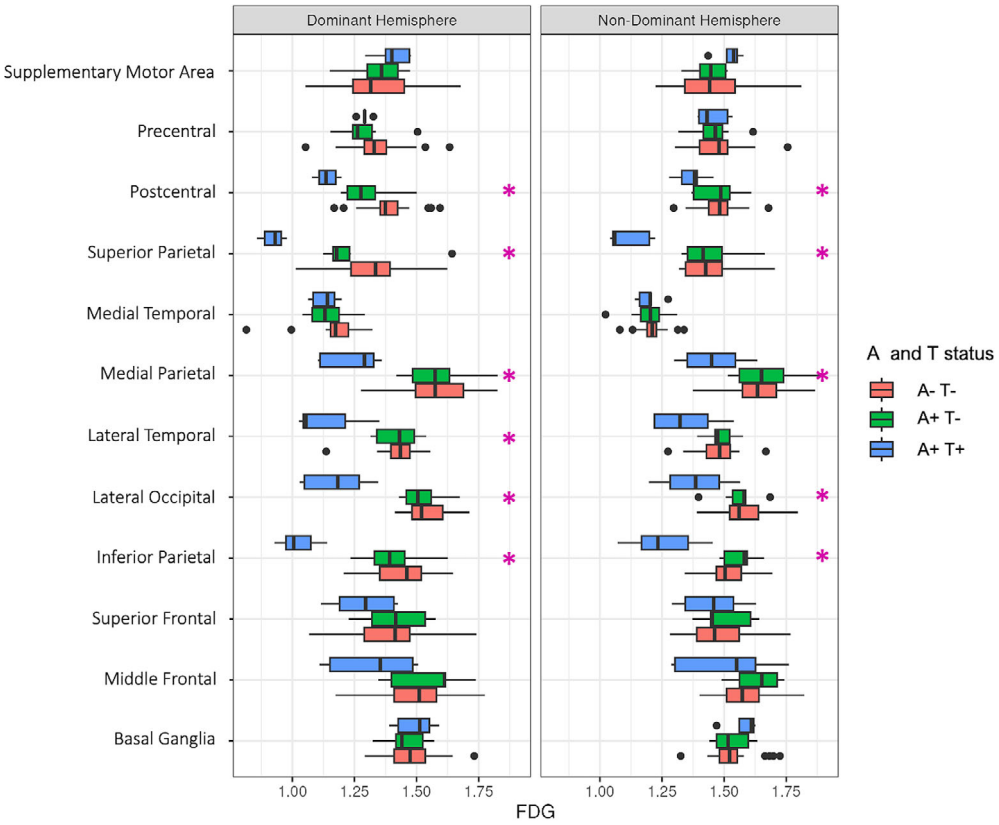

FIGURE 4 FDG uptake across different brain regions in CBS patients according to A/T status. Boxplots of FDG uptake (*x*-axis) according to A/T status (orange: A-T-; green: A+T-; blue: A+T+) determined by PiB and flortaucipir PET. Data are shown per each hemisphere (dominant and non-dominant). Pink asterisks highlight significant differences. CBS, corticobasal syndrome; FDG, [18F] fluorodeoxyglucose; PET, positron emission tomography; PiB, Pittsburg compound B.

dinal cognitive decline in individuals of 50–90 years of age and CSF tau and phospho-tau (T+) but only when β-amyloid was also decreased (A+), implying that cortical dysfunction is affected by the presence of both A and T positivity.[42] However, a different study showed that cortical hypometabolism in retrosplenial and parietal cortices in a group of AD patients was only associated with structural atrophy and tau pathology but not β-amyloid pathology.[43] Given that only A+ patients also showed T+, it is possible that tau plays a dominant role in determining hypometabolism in our CBS cohort. Overall, our FDG-PET asymmetry index was useful in separating A+T+ CBS patients and should be validated in independent cohorts to assess its feasibility as a biomarker of AD pathology in future therapeutic trials for CBS.[3,12,39] Of note, no CBS patient had a positive tau status in the absence of β-amyloid.

It has been previously demonstrated that flortaucipir uptake is not elevated in patients with primary age-related tauopathy (PART),[15,16] an age-related 3R+4R tauopathy characterized by the presence of tangles in the absence of, or minimal, β-amyloid pathology. However, flortaucipir PET is able to detect AD-related tau (3R+4R) in patients with a Braak stage V or VI in patients with different primary pathologies, including AD, pathological aging, and Lewy body disease.[15,16] PART is often observed in CBS patients at autopsy; therefore, the absence of CBS patients with an A-T+ status likely reflects flortaucipir insensitivity to detecting PART.

Clinically, we observed worse WAB praxis scores in the A+ CBS patients, consistent with prior reports in which ideomotor apraxia was reported as predominant in CBS-AD patients.[3,6] The A+T+ patients showed worse performance on both WAB praxis and the MoCA, although we did not observe significant differences across the AT groups. The relatively poor performance of the A+T- patients could have been due to their older age.[2] Another possibility is that, because the A+T+ patients are younger, their cognitive reserve masked the effects of the combined pathologies. This is consistent with the result reported by Boyd et al. in which patients with CBS-AD had a younger onset compared to CBS-non-AD.[5]

The strengths of this study include the dual characterization of our cohort with both PiB and FTP PET, along with a comprehensive standardized clinical, neuropsychological, and speech assessment. Furthermore, each result was corrected for age, further supporting that the alterations in metabolism in our CBS cohort were the result of amyloid and tau pathology. A limitation of this study is the absence of autopsy confirmation of AD pathology. Further studies with proven *post mortem* pathology are warranted to confirm our results. Another potential limitation is that we utilized a temporal lobe meta-ROI to

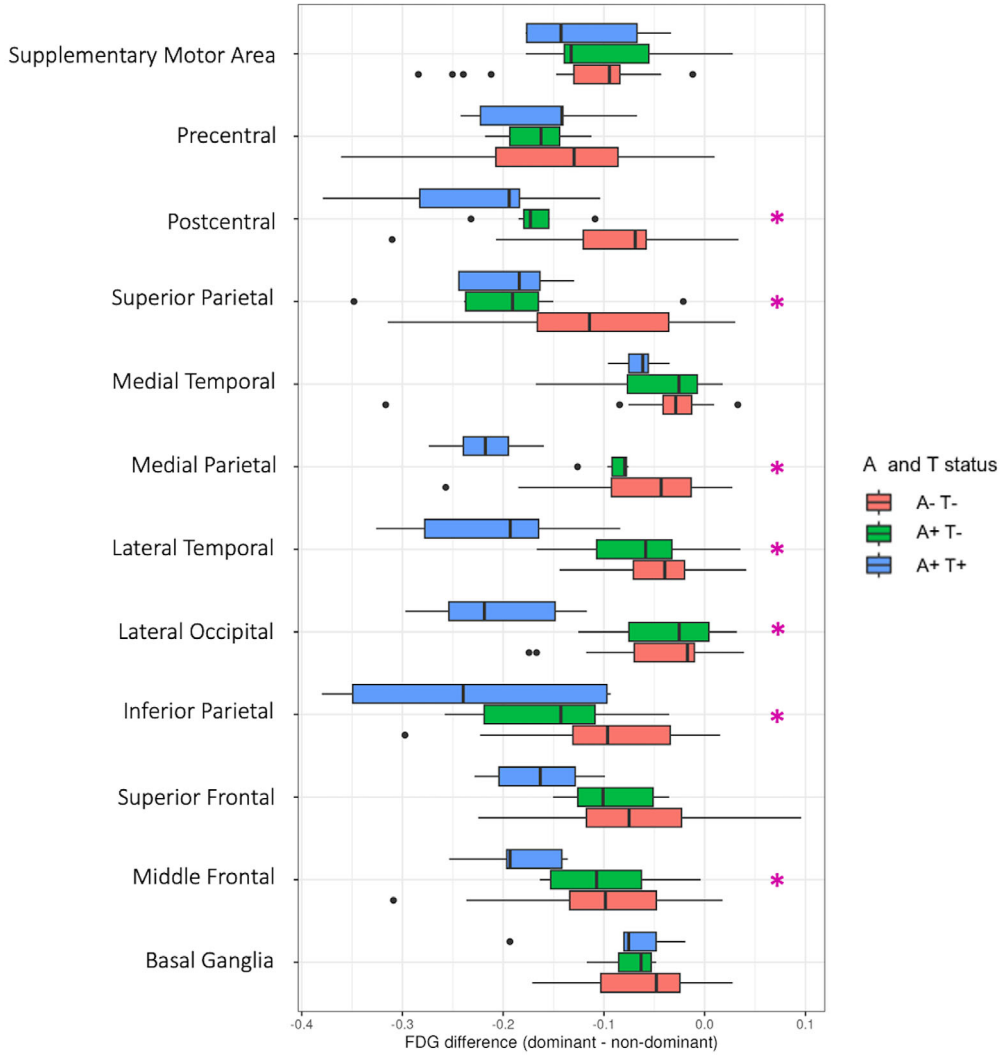

FIGURE 5 Asymmetry of FDG uptake in CBS patients according to A/T status. Boxplots represent the difference in FDG uptake (dominant–non-dominant hemisphere) according to A/T status (orange: A-T-; green: A+T-; blue: A+T+) determined at PiB and flortaucipir PET. Pink asterisks highlight significant differences. CBS, corticobasal syndrome; FDG, [18F] fluorodeoxyglucose; PET, positron emission tomography; PiB, Pittsburg compound B.

define T status, which included medial temporal regions that are typically spared in CBS-AD.[24,39] This is most likely the reason no A-T+ patient was detected. Indeed, the T status limitedly refers to temporal tau, not including premotor/motor cortices that are expected to be affected by CBD pathology. The AD-specific temporal ROI that was adopted for this study has therefore possibly limited the detection of those cases. Still, absence of beta-amyloid with temporal tau (PART) can be observed in 4R tauopathies such as CBD, but no case of PART was detected in our cohort. Furthermore, this was a single-center study, and our cohort was of a relatively small number. Therefore, replication in other centers' cohorts would increase generalizability and validate our findings.

For therapies to be applied in CBS, it is critically important to identify its underlying pathology *ante mortem*. The CSF 4R-tau biomarker MTBR-tau proved useful in differentiating CBD pathology from controls.[44] Still, longitudinal invasive tests to test a drug's efficacy could expose patients to several risks. A breakthrough in the treatment of AD came when PiB PET allowed for reliable assessment of levels of brain β-amyloid longitudinally. The same reasoning cannot be applied to CBS, with AD only responsible for approximately 30% of all cases.[3–8] However, patients with atypical AD are starting to be considered as candidates for monoclonal anti-amyloid antibodies like lecanemab,[45] highlighting the importance of discovering noninvasive biomarkers for AD in the CBS population. We therefore propose FDG PET to be a useful tool in detecting CBS patients with the classical AD signature, that is, carrying an A+T+ status, where it showed a signature of more accentuated and asymmetrical temporo-parieto-occipital hypometabolism. Its utility, however, was only limited in distinguishing A-T- cases from A+T- cases, and we warrant care in interpretation in those cases. Molecular PET could be a valid alternative to CSF testing to demonstrate AD pathology and find patients eligible to receive anti-amyloid treatment. Given the absence of A-T+ patients in our cohort,

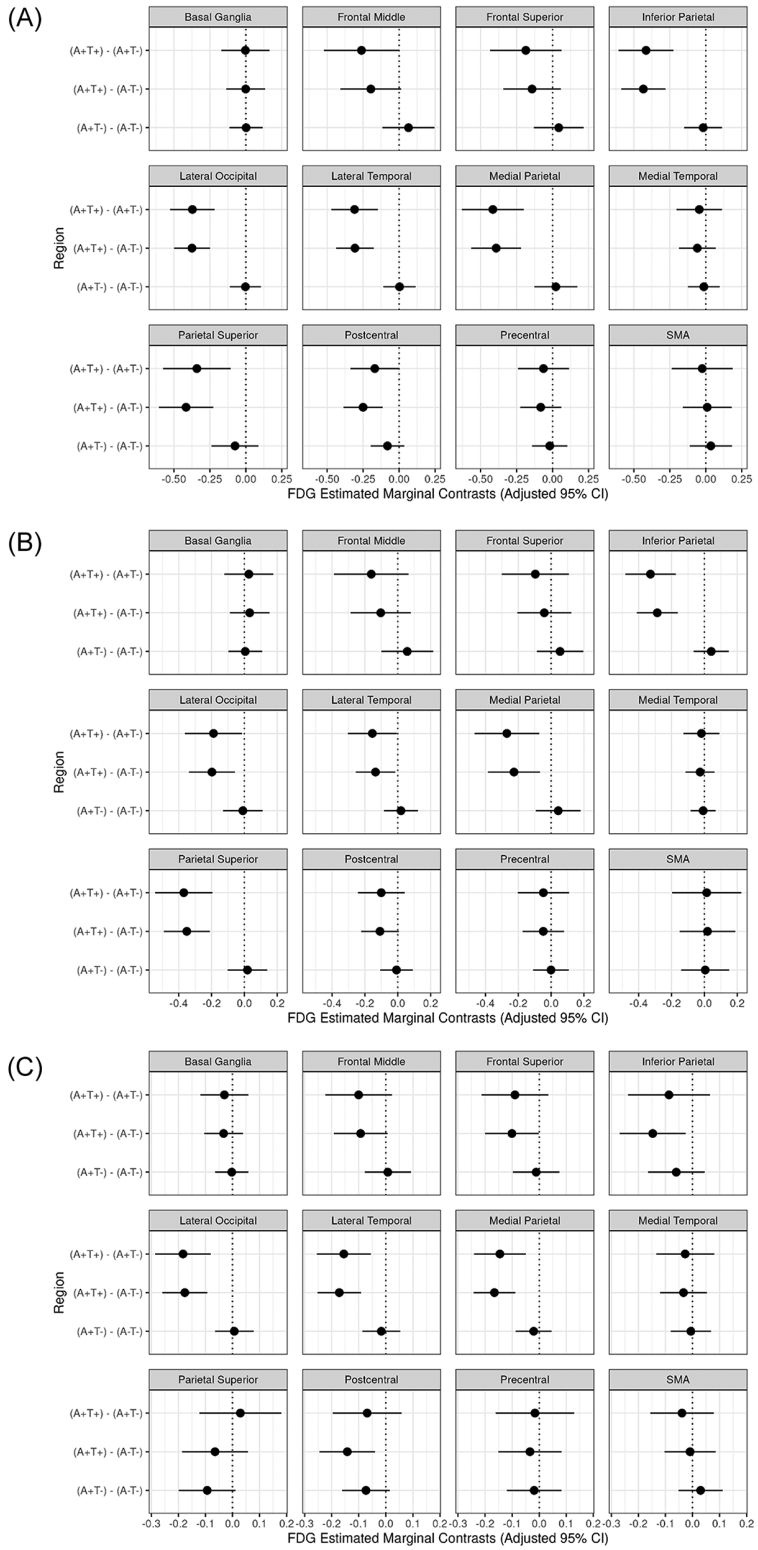

FIGURE 6 Estimated marginal mean model accounting for the effect of age, A and T status on FDG uptake. (A) Dominant hemisphere age-adjusted FDG estimated marginal contrasts. (B) Non-dominant hemisphere age-adjusted FDG estimated marginal contrasts. (C) Asymmetry index age-adjusted FDG estimated marginal contrasts. FDG, [18F] fluorodeoxyglucose.

the use of FTP PET alone might be better in discriminating CBS-AD patients, as it would be potentially more specific in detecting patients with a higher Braak stage. We show the utility of a combination of FDG, β-amyloid, and tau PET in the stratification of CBS patients, but further studies validating their usefulness in comparing *post mortem* pathology are warranted.

5 | CONCLUSIONS

We have demonstrated that β-amyloid and tau PET, rather than β-amyloid alone, should be used to identify CBS patients with AD patterns of hypometabolism. Hypometabolism becomes more severe, widespread, and lateralized at a single-patient level as β-amyloid and

tau synergistically act on the neurodegenerative processes. Further studies with larger cohorts will be necessary to determine whether a single FDG PET could alone predict A and T statuses of these patients, but this study sets the path for the use of FDG PET as a biomarker in CBS that could be used as a potential tool to enroll CBS patients into clinical trials. Asymmetry at FDG PET and a pattern of hypometabolism that includes lateral temporal and parieto-occipital lobes should be further investigated as a non-invasive and accessible biomarker of CBS-AD.

ACKNOWLEDGMENTS

We thank all the patients and their families for their commitment. The study was funded by NIH grants R01-AG50603, R01-NS112153 and R01-NS89757.

CONFLICT OF INTEREST STATEMENT

A. Ghirelli, A. W. Goodrich, Y. C. Stephens, F. Ali, M. Machulda, M. L. Senjem, V. J. Lowe, C. R. Jack Jr. have nothing to disclose. C. Schwarz receives fundings by the NIH. J. Graff-Radford receives fundings by the NIH, DSMB for NINDS strokeNET, he is site-investigator for trials sponsored by Eisai and Cognition therapeutics, he received honoraria from the American Academy of Neurology for development of educational courses. M. Filippi is editor-in-chief of the *Journal of Neurology*, associate editor of *Human Brain Mapping*, *Neurological Sciences*, and *Radiology*; received compensation for consulting services from Alexion, Almirall, Biogen, Merck, Novartis, Roche, Sanofi; speaking activities from Bayer, Biogen, Celgene, Chiesi Italia SpA, Eli Lilly, Genzyme, Janssen, Merck-Serono, Neopharmed Gentili, Novartis, Novo Nordisk, Roche, Sanofi, Takeda, and TEVA; participation in Advisory Boards for Alexion, Biogen, Bristol-Myers Squibb, Merck, Novartis, Roche, Sanofi, Sanofi-Aventis, Sanofi-Genzyme, Takeda; scientific direction of educational events for Biogen, Merck, Roche, Celgene, Bristol-Myers Squibb, Lilly, Novartis, Sanofi-Genzyme; he receives research support from Biogen Idec, Merck-Serono, Novartis, Roche, the Italian Ministry of Health, the Italian Ministry of University and Research, and Fondazione Italiana Sclerosi Multipla. F. Agosta is associate editor of *NeuroImage: Clinical*, has received speaker honoraria from Biogen Idec, Italfarmaco, Roche, Zambon and Eli Lilly, and receives or has received research supports from the Italian Ministry of Health, the Italian Ministry of University and Research, AriSLA (Fondazione Italiana di Ricerca per la SLA), the European Research Council, the EU Joint Programme – Neurodegenerative Disease Research (JPND), and Foundation Research on Alzheimer Disease (France). K. Josephs is associate editor of *Annals of Clinical and Translational Neurology* and serves on the editorial board of *Acta Neuropathologica* and *Journal of Neurology*. Author disclosures are available in the Supporting Information.

DATA AVAILABILITY STATEMENT

The dataset used for this study will be made available by the corresponding author on request to qualified researchers.

ETHICS STATEMENT

The study was approved by the Mayo Clinic IRB. Informed consent was obtained from all patients to participate in this study.

ORCID

Alma Ghirelli https://orcid.org/0000-0001-8440-1036

REFERENCES

1. Armstrong MJ, Litvan I, Lang AE, et al. Criteria for the diagnosis of corticobasal degeneration. *Neurology*. 2013;80(5):496-503.
2. Koga S, Josephs KA, Aiba I, Yoshida M, Dickson DW Neuropathology and emerging biomarkers in corticobasal syndrome. *J Neurol Neurosurg Psychiatry*. 2022;93(9):919-929.
3. Shir D, Pham NTT, Botha H, et al. Clinicoradiologic and neuropathologic evaluation of corticobasal syndrome. *Neurology*. 2023;101(3):e289-e299.
4. Ouchi H, Toyoshima Y, Tada M, et al. Pathology and sensitivity of current clinical criteria in corticobasal syndrome. *Mov Disord*. 2014;29(2):238-244.
5. Boyd CD, Tierney M, Wassermann EM, et al. Visuoperception test predicts pathologic diagnosis of Alzheimer disease in corticobasal syndrome. *Neurology*. 2014;83(6):510-519.
6. Lee SE, Rabinovici GD, Mayo MC, et al. Clinicopathological correlations in corticobasal degeneration. *Ann Neurol*. 2011;70(2):327-340.
7. Ling H, O'sullivan SS, Holton JL, et al. Does corticobasal degeneration exist? A clinicopathological re-evaluation. *Brain*. 2010;133(Pt 7):2045-2057.
8. Shelley BP, Hodges JR, Kipps CM, Xuereb JH, Bak TH Is the pathology of corticobasal syndrome predictable in life? *Mov Disord*. 2009;24(11):1593-1599.
9. Sakae N, Josephs KA, Litvan I, et al. Clinicopathologic subtype of Alzheimer's disease presenting as corticobasal syndrome. *Alzheimers Dement*. 2019;15(9):1218-1228.
10. Di Stasio F, Suppa A, Marsili L, et al. Corticobasal syndrome: neuroimaging and neurophysiological advances. *Eur J Neurol*. 2019;26(5):701-e52.
11. Whitwell JL, Jack CR, Boeve BF, et al. Imaging correlates of pathology in corticobasal syndrome. *Neurology*. 2010;75(21):1879-1887.
12. Hu WT, Rippon GW, Boeve BF, et al. Alzheimer's disease and corticobasal degeneration presenting as corticobasal syndrome. *Mov Disord*. 2009;24(9):1375-1379.
13. Parmera JB, Coutinho AM, Aranha MR, et al. FDG-PET patterns predict amyloid deposition and clinical profile in corticobasal syndrome. *Mov Disord*. 2021;36(3):651-661.
14. Sha SJ, Ghosh PM, Lee SE, et al. Predicting amyloid status in corticobasal syndrome using modified clinical criteria, magnetic resonance imaging and fluorodeoxyglucose positron emission tomography. *Alzheimers Res Ther*. 2015;7(1):8.
15. Lowe VJ, Lundt ES, Albertson SM, et al. Tau-positron emission tomography correlates with neuropathology findings. *Alzheimers Dement*. 2020;16(3):561-571.
16. Ghirelli A, Tosakulwong N, Weigand SD, et al. Sensitivity-specificity of tau and amyloid β positron emission tomography in frontotemporal lobar degeneration. *Ann Neurol*. 2020;88(5):1009-1022.
17. Lowe VJ, Curran G, Fang P, et al. An autoradiographic evaluation of AV-1451 Tau PET in dementia. *Acta Neuropathol Commun*. 2016;4(1):58.
18. Marquié M, Normandin MD, Vanderburg CR, et al. Validating novel tau positron emission tomography tracer [F-18]-AV-1451 (T807) on postmortem brain tissue. *Ann Neurol*. 2015;78(5):787-800.

19. Niccolini F, Wilson H, Hirschbichler S, et al. Disease-related patterns of in vivo pathology in Corticobasal syndrome. *Eur J Nucl Med Mol Imaging*. 2018;45(13):2413-2425.
20. Cho H, Baek MS, Choi JY, et al. (18)F-AV-1451 binds to motor-related subcortical gray and white matter in corticobasal syndrome. *Neurology*. 2017;89(11):1170-1178.
21. Nakano Y, Shimada H, Shinotoh H, et al. PET-based classification of corticobasal syndrome. *Parkinsonism Relat Disord*. 2022;98:92-98.
22. Jack CR, Wiste HJ, Botha H, et al. The bivariate distribution of amyloid-β and tau: relationship with established neurocognitive clinical syndromes. *Brain*. 2019;142(10):3230-3242.
23. Palleis C, Brendel M, Finze A, et al. Cortical [(18) F]PI-2620 binding differentiates corticobasal syndrome subtypes. *Mov Disord*. 2021;36(9):2104-2115.
24. Ali F, Whitwell JL, Martin PR, et al. [(18)F] AV-1451 uptake in corticobasal syndrome: the influence of beta-amyloid and clinical presentation. *J Neurol*. 2018;265(5):1079-1088.
25. Goetz CG, Tilley BC, Shaftman SR, et al. Movement disorder society-sponsored revision of the unified Parkinson's disease rating scale (MDS-UPDRS): scale presentation and clinimetric testing results. *Mov Disord*. 2008;23(15):2129-2170.
26. Whitwell JL, Master AV, Avula R, et al. Clinical correlates of white matter tract degeneration in progressive supranuclear palsy. *Arch Neurol*. 2011;68(6):753-760.
27. Vanbellingen T, Kersten B, Van Hemelrijk B, et al. Comprehensive assessment of gesture production: a new test of upper limb apraxia (TULIA). *Eur J Neurol*. 2010;17(1):59-66.
28. Kertesz A. *Western Aphasia Battery–Revised*. PsychCorp; 2007.
29. Nasreddine ZS, Phillips NA, Bédirian V, et al. The Montreal Cognitive Assessment, MoCA: a brief screening tool for mild cognitive impairment. *J Am Geriatr Soc*. 2005;53(4):695-699.
30. Warrington E. *The Camden Memory Test Battery*. Psychology Press; 1996.
31. Warrington EK. *Visual Object and Space Perception Battery*. Thames Valley Test Company; 1991.
32. Buciuc M, Botha H, Murray ME, et al. Utility of FDG-PET in diagnosis of Alzheimer-related TDP-43 proteinopathy. *Neurology*. 2020;95(1):e23-e34.
33. Whitwell JL, Ahlskog JE, Tosakulwong N, et al. Pittsburgh compound B and AV-1451 positron emission tomography assessment of molecular pathologies of Alzheimer's disease in progressive supranuclear palsy. *Parkinsonism Relat Disord*. 2018;48:3-9.
34. Klunk WE, Koeppe RA, Price JC, et al. The centiloid project: standardizing quantitative amyloid plaque estimation by PET. *Alzheimers Dement*. 2015;11(1):1-15.e1-4.
35. Jack CR, Wiste HJ, Weigand SD, et al. Defining imaging biomarker cut points for brain aging and Alzheimer's disease. *Alzheimers Dement*. 2017;13(3):205-216.
36. Goodheart AE, Locascio JJ, Samore WR, et al. 18F-AV-1451 positron emission tomography in neuropathological substrates of corticobasal syndrome. *Brain*. 2021;144(1):266-277.
37. Jack CR, Wiste HJ, Algeciras-Schimnich A, et al. Predicting amyloid PET and tau PET stages with plasma biomarkers. *Brain*. 2023;146(5):2029-2044.
38. Ashburner J, Friston KJ. Unified segmentation. *Neuroimage*. 2005;26(3):839-851.
39. Cerami C, Dodich A, Iannaccone S, et al. Individual brain metabolic signatures in corticobasal syndrome. *J Alzheimers Dis*. 2020;76(2):517-528.
40. Dickson DW, Crystal HA, Mattiace LA, et al. Identification of normal and pathological aging in prospectively studied nondemented elderly humans. *Neurobiol Aging*. 1992;13(1):179-189.
41. Hanseeuw BJ, Betensky RA, Schultz AP, et al. Fluorodeoxyglucose metabolism associated with tau-amyloid interaction predicts memory decline. *Ann Neurol*. 2017;81(4):583-596.
42. Timmers M, Tesseur I, Bogert J, et al. Relevance of the interplay between amyloid and tau for cognitive impairment in early Alzheimer's disease. *Neurobiol Aging*. 2019;79:131-141.
43. Strom A, Iaccarino L, Edwards L, et al. Cortical hypometabolism reflects local atrophy and tau pathology in symptomatic Alzheimer's disease. *Brain*. 2022;145(2):713-728.
44. Horie K, Barthélemy NR, Spina S, et al. CSF tau microtubule-binding region identifies pathological changes in primary tauopathies. *Nat Med*. 2022;28(12):2547-2554.
45. Cummings J, Apostolova L, Rabinovici GD, et al. Lecanemab: appropriate use recommendations. *J Prev Alzheimers Dis*. 2023;10(3):362-377.

SUPPORTING INFORMATION

Additional supporting information can be found online in the Supporting Information section at the end of this article.

How to cite this article: Ghirelli A, Goodrich AW, Stephens YC, et al. Relationships between hypometabolism and both β-amyloid and tau PET in corticobasal syndrome. *Alzheimer's Dement*. 2025;21:e70018. https://doi.org/10.1002/alz.70018